

## Ca(BH<sub>4</sub>)<sub>2</sub>-MgF<sub>2</sub> Reversible Hydrogen Storage: Reaction Mechanisms and Kinetic Properties

Rapee Gosalawit-Utke<sup>1,\*</sup>, Karina Suarez<sup>1</sup>, Jose M. Bellosta von Colbe<sup>1</sup>, Ulrike Bösenberg<sup>1</sup>, Torben R. Jensen<sup>2</sup>, Yngve Cerenius<sup>3</sup>, Christian Bonatto Minella<sup>1</sup>, Claudio Pistidda<sup>1</sup>, Gagik Barkhordarian<sup>1</sup>, Matthias Schulze<sup>4</sup>, Thomas Klassen<sup>1</sup>, Rüdiger Bormann<sup>1</sup>, Martin Dornheim<sup>1</sup>

<sup>1</sup>Institute of Materials Research, Materials Technology, Helmholtz-Zentrum Geesthacht, Zentrum für Material-und Küstenforschung, D-21502 Geesthacht, Germany, Email: rapee.gosalawit@gkss.de.

<sup>2</sup>Center for Energy Materials, iNANO and Department of Chemistry, University of Aarhus, Langelandsgade 140, DK-8000 Aarhus C, Denmark.

<sup>3</sup>MaXLAB, Lund University, S-22100 Lund, Sweden.

<sup>4</sup>Institute of Material Technology, Helmut-Schmidt-University, University of the Federal Armed Forces Hamburg, Holstenhofweg 85, D-22043 Hamburg, Germany.

A composite of Ca(BH<sub>4</sub>)<sub>2</sub>-MgF<sub>2</sub> is proposed as a reversible hydrogen storage system. The dehydrogenation and rehydrogenation reaction mechanisms are investigated by *in situ* time-resolved synchrotron radiation powder X-ray diffraction (SR-PXD) and raman spectroscopy. The formation of an intermediate phase (CaF<sub>2-x</sub>H<sub>x</sub>) is observed during rehydrogenation. The hydrogen content of 4.3 wt. % is obtained within 4 h during the 1<sup>st</sup> dehydrogenation at isothermal and isobaric condition of 330 °C and 0.5 bar H<sub>2</sub>, respectively. The cycling efficiency is evaluated by three release and uptake cycles together with absorbed hydrogen content in the range of 5.1-5.8 wt. % after 2.5 h (T=330 °C and *p*(H<sub>2</sub>)=130 bar). The kinetic properties on the basis of hydrogen absorption are comparable for all cycles. As compared to pure Ca(BH<sub>4</sub>)<sub>2</sub> and Ca(BH<sub>4</sub>)<sub>2</sub>-MgH<sub>2</sub> composite, Ca(BH<sub>4</sub>)<sub>2</sub>-MgF<sub>2</sub> composite reveals the kinetic destabilization and the reproducibility of hydrogen storage capacities during cycling, respectively.

\* Corresponding author

Keywords: Hydrogen storage material, Metal hydride, X-ray diffraction, calciumborohydride, Synchrotron XRD

## 1. Introduction

Owing to the guidelines defined by the U.S. Department of Energy (DOE), hydrogen storage systems with a target of 6 wt. % hydrogen content and desorption of hydrogen at 1 bar below 85 °C, corresponding to a formation enthalpy of  $\sim -47$  kJ/mol H<sub>2</sub>, are required for fuel cell powered vehicles to be able to replace petroleum-fueled vehicles on a large scale [1-2]. Metal hydrides, e.g. alanates [3], amides [4], and borohydrides [5], are the most promising candidates for hydrogen storage systems due to their safety, light weight, and compact size as well as highest storage capacity by volume as compared to compressed or liquid hydrogen system.

One of the most interesting compounds with a high hydrogen storage density is Ca(BH<sub>4</sub>)<sub>2</sub> containing theoretically 11.6 wt.% H<sub>2</sub> capacity. As compared to LiBH<sub>4</sub>, although the hydrogen storage capacity of Ca(BH<sub>4</sub>)<sub>2</sub> is less than that of LiBH<sub>4</sub>, it has still high theoretical capacity (11.6 wt.%) enough to reach the target of DOE (9 wt. %), and has lower dehydrogenation temperature than LiBH<sub>4</sub> [6]. Calcium borohydride can be prepared by several reactions, for example, (i) calcium hydride [7] or alkoxide [8] with diborane; (ii) reaction in tetrahydrofuran (THF) [9], forming Ca(BH<sub>4</sub>)<sub>2</sub>-THF, which is commercially available. Regarding to the structure of known Ca(BH<sub>4</sub>)<sub>2</sub> polymorphs, *Fddd* structure of  $\alpha$ -Ca(BH<sub>4</sub>)<sub>2</sub> was presented in 2006 [10]; thereafter an alternative structure of *F2dd* symmetry for  $\alpha$ -Ca(BH<sub>4</sub>)<sub>2</sub> was proposed [11-12]. In the case of  $\beta$ -Ca(BH<sub>4</sub>)<sub>2</sub>, several structures were revealed such as *P4<sub>2</sub>/m*, *P4<sub>2</sub>* and *P4* symmetries [13-15]. Interestingly, it was found that  $\alpha$ -Ca(BH<sub>4</sub>)<sub>2</sub> transformed to an  $\alpha'$ -Ca(BH<sub>4</sub>)<sub>2</sub> (*I42d* symmetry) at elevated temperature, before transforming completely to  $\beta$ -Ca(BH<sub>4</sub>)<sub>2</sub> [11, 15]. Moreover, an  $\gamma$ -Ca(BH<sub>4</sub>)<sub>2</sub> with *Pbca* structure was also exposed as a dynamically stable and non-experimental phase [11]. The primary and most likely hydrogen desorption pathways of Ca(BH<sub>4</sub>)<sub>2</sub> are the following:



Earnest consideration of Ca(BH<sub>4</sub>)<sub>2</sub> as a hydrogen storage was exposed in 2006 by Miwa et al. [10]. They found that the complete dehydrogenation of Ca(BH<sub>4</sub>)<sub>2</sub> as in Eq. (1) required an enthalpy of 151 kJ/mol H<sub>2</sub>. The next-highest hydrogen capacity decomposing to CaB<sub>6</sub> and CaH<sub>2</sub> (Eq. (2)) required 32-38 kJ/mol H<sub>2</sub> [16-18], while that of Eq. (3) was 56 kJ/mol H<sub>2</sub> [18]. However, it is not clear which

dehydrogenation reaction the  $\text{Ca}(\text{BH}_4)_2$  system takes. A number of studies showed the formation of  $\text{CaH}_2$  during dehydrogenation reaction [19-21]. Besides, some reports have indicated that they were the  $\beta$  and  $\gamma$  forms of  $\text{Ca}(\text{BH}_4)_2$  decomposing, which the dehydrogenation was a two-step process [17, 19-20]. There were also experimental evidences that a number of intermediates and products; that is,  $\text{CaB}_2\text{H}_x$  [20],  $\text{CaB}_6$  [22],  $\text{CaB}_{12}\text{H}_{12}$  [17], and orthorhombic [21] and amorphous [17] phases, existed during dehydrogenation. Kim et al. [22] claimed that the formation of  $\text{CaB}_6$  instead of amorphous boron can be an important factor in reversibility of  $\text{Ca}(\text{BH}_4)_2$  as is the case for  $\text{LiBH}_4+\text{CaH}_2$  versus pure  $\text{LiBH}_4$ .

With respect to the significant hydrogen content released,  $\text{Ca}(\text{BH}_4)_2$  seems to be a suitable material for hydrogen storage system. However, its sluggish kinetics especially during rehydrogenation still impedes the practical uses of this material. For instant, Kim et al. [22] revealed that almost negligible rehydrogenation of pure  $\text{Ca}(\text{BH}_4)_2$  occurred after 24 h under 90 bar  $\text{H}_2$  and at 350 °C. Moreover, Rönnebro et al. [23] found that the hydrogenation of  $\text{CaB}_6$  and  $\text{CaH}_2$  to produce  $\text{Ca}(\text{BH}_4)_2$  could not be succeeded without 4-8 wt.% of additives ( $\text{TiCl}_3$  and Pd) although it was carried out at high temperature and pressure ( $T=400-440$  °C and  $p(\text{H}_2)=700$  bar). Therefore, improving the kinetic properties of  $\text{Ca}(\text{BH}_4)_2$  under practical temperature and pressure conditions is currently a main goal.

First approach is the system with several reacting components (reactive hydride composites (RHCs)) [24]. For example,  $\text{Ca}(\text{BH}_4)_2\text{-MgH}_2$  composite decomposed in two steps; that is, (i) at 360 °C,  $\text{Ca}(\text{BH}_4)_2\text{-MgH}_2$  generated  $\text{CaH}_2$ , Mg, B (or  $\text{MgB}_2$ ) and an intermediate compound of  $\text{Ca}_3\text{Mg}_4\text{H}_{14}$ ; and (ii) at 400 °C  $\text{Ca}_3\text{Mg}_4\text{H}_{14}$  dehydrogenated to obtain  $\text{CaH}_2$  and Mg [25]. However, it should be noted that  $\text{Ca}(\text{BH}_4)_2\text{-MgH}_2$  composite gave only 60% reversibility after rehydrogenation for 24 h under 90 bar  $\text{H}_2$  at 350 °C [22]. The second considerable approach is to catalyze  $\text{Ca}(\text{BH}_4)_2$  with a small amount (~ 2 mol %) of various fluorine and chlorine compounds [6, 26]. The dehydrogenation temperature of  $\text{TiCl}_3$ -catalyzed  $\text{Ca}(\text{BH}_4)_2$  decreased approximately 50 °C, however, its hydrogen content rehydrogenated under 90 bar  $\text{H}_2$  at 350 °C for 24 h was only 3.8 wt. % [26]. Among all catalysts ( $\text{TiF}_3$ ,  $\text{TiCl}_3$ ,  $\text{NbF}_5$  and  $\text{NbCl}_5$ ), Kim et al. [6] reported that  $\text{NbF}_5$  exhibited the best performance. Not only the reduction in dehydrogenation temperature of  $\text{Ca}(\text{BH}_4)_2$  as in the case of  $\text{TiCl}_3$  was obtained, but the hydrogen content reabsorbed at 420 °C under 90 bar  $\text{H}_2$  for 24 h of  $\text{NbF}_5$ -catalyzed  $\text{Ca}(\text{BH}_4)_2$  also enhanced up to 5 wt. % [6]. Although many studies have focused on the catalytic properties of the transition metals, fluorides also appear to play an important role. Here we consider the inclusion of fluorine as a major composite constituent.

In the present work, the composite of  $\text{Ca}(\text{BH}_4)_2\text{-MgF}_2$  was created based on the combination of two strategies; that is, (i) RHCs; and (ii) metal-fluorine catalyzed- $\text{Ca}(\text{BH}_4)_2$ , to destabilize the kinetics of  $\text{Ca}(\text{BH}_4)_2$ . In order to reveal the kinetic improvement, the performance of  $\text{Ca}(\text{BH}_4)_2\text{-MgF}_2$  composite was compare to that of pure  $\text{Ca}(\text{BH}_4)_2$ , metal-fluorine ( $\text{NbF}_5$ ) catalyzed- $\text{Ca}(\text{BH}_4)_2$  and  $\text{Ca}(\text{BH}_4)_2\text{-MgH}_2$

composite. Importantly, this composite is not yet reported. *In situ* time-resolved synchrotron radiation powder X-ray diffraction (SR-PXD) and raman spectroscopy were performed to determine the reaction mechanisms from the structural point of view during dehydrogenation and rehydrogenation of Ca(BH<sub>4</sub>)<sub>2</sub>-MgF<sub>2</sub> composite. The kinetic properties and cycling efficiency were evaluated by a continuously performed DSC-TG-MS and a Sieverts'-type apparatus.

## 2. Experimental details

Ca(BH<sub>4</sub>)<sub>2</sub>·2THF was purchased from Sigma-Aldrich Chemie GmbH, Steinheim, Germany. MgF<sub>2</sub> (99.9 %, Ca+Na < 1 %) was bought from Alfa Aesar, Karlsruhe, Germany. Ca(BH<sub>4</sub>)<sub>2</sub> was prepared by drying the commercial Ca(BH<sub>4</sub>)<sub>2</sub>·2THF at 200 °C under vacuum for 1.25 h. Dried Ca(BH<sub>4</sub>)<sub>2</sub> and MgF<sub>2</sub> in the molar ratio of 1:1 were milled in stainless steel vials for 5 h using a Spex 8000 M Mixer Mill under argon atmosphere. The milling was carried out using 10 mm stainless steel balls with a ball-to-powder ratio (BPR) of 10:1.

Differential scanning calorimetry (DSC) and thermo-gravimetric analysis (TGA) were carried out simultaneously by a Netzsch STA 409 under argon atmosphere. The milled Ca(BH<sub>4</sub>)<sub>2</sub>-MgF<sub>2</sub> was heated from room temperature (~ 20 °C) to 500 °C with the heating rate of 5 K/min under an argon flow of 150 ml/min. The concentration of HF, BF<sub>3</sub>, B<sub>2</sub>H<sub>6</sub>, H<sub>2</sub>, and H<sub>2</sub>O in the exhaust gas was continuously evaluated by a Hiden HPR-20 QIC mass spectrometer (MS).

Dried Ca(BH<sub>4</sub>)<sub>2</sub> was characterized by x-ray diffraction (XRD) using a Bruker axs with Cu K $\alpha$  radiation ( $\lambda=1.5406$  Å). The diffraction patterns were collected in the range of 10-55° (2 $\theta$ ) and in the step of 0.05°. The powders were protected from air and humidity by polyimide film (kapton foil).

Raman spectroscopy was detected by an Alpha 300 from WITec, Ulm, Germany. The measurements were carried out with the center and laser wavelengths of 696.794 and 532 nm, respectively. The integration time and accumulation of the single scan were 2 s and 40, respectively. The powder samples were filled into quartz cell using a SUPRASIL® 400  $\mu$ m with a PTFE-stopper (Mikro-Küvette 115 F-QS, 10×2 mm).

*In situ* time-resolved synchrotron radiation powder X-ray diffraction (SR-PXD) was performed at the MAX II Synchrotron at beamline I711, Lund, Sweden [27]. A Mar165 CCD detector was exposure 30 s with a selected X-ray wavelength of 1.09801 and 1.072 Å for each diffraction pattern. The powders were encapsulated into airtight sapphire capillaries in an argon glovebox. The hydrogen pressure was kept constant during the experiments. The sample was heated by a tungsten wire wrapped around the capillary while the temperature was controlled by the external PID regulator and thermocouple inserted into the powder-bed as a schematic draw shown elsewhere [28]. The

experiments were carried out in the temperature range of 25-390 °C (vacuum) and 25-380 °C (100 bar H<sub>2</sub>) for dehydrogenation and hydrogenation, respectively.

Dehydrogenation, rehydrogenation and cycling efficiency were carried out by a carefully calibrated Sievert's-type apparatus using a PCTPro-2000 (Hy-Energy LLC). The powder samples were filled in a high pressure-temperature vessel under argon atmosphere. All the powder samples were heated up and kept under isothermal and isobaric conditions of 330 °C (0.5 bar H<sub>2</sub>) and 330 °C (130 bar H<sub>2</sub>) for dehydrogenation and rehydrogenation, respectively. The hydrogen desorption and absorption was firstly determined when the isothermal and isobaric conditions were reached.

### 3. Results and discussion

#### 3.1. Dehydrogenation of Ca(BH<sub>4</sub>)<sub>2</sub>-MgF<sub>2</sub> composite

In order to preliminarily determine the dehydrogenation temperature and hydrogen content released, milled Ca(BH<sub>4</sub>)<sub>2</sub>-MgF<sub>2</sub> was investigated by a simultaneously performed DSC-TG-MS measurements. In a previous study [25], an endothermic peak at about 130 °C corresponding to the polymorphic transformation from  $\alpha$ - to  $\beta$ -Ca(BH<sub>4</sub>)<sub>2</sub> was reported. However, this transformation is not significantly obvious in our DSC curve (Fig.1). This could be due to the fact that the mixture of  $\alpha$ - and  $\beta$ -Ca(BH<sub>4</sub>)<sub>2</sub> was obtained after drying instead of pure  $\alpha$ -Ca(BH<sub>4</sub>)<sub>2</sub> as previously discussed by Kim et al. [22]. From Fig. 1, the DSC curve shows an endothermic peak together with a strong hydrogen signal (MS result) at around 390 °C indicating the dehydrogenation of Ca(BH<sub>4</sub>)<sub>2</sub>-MgF<sub>2</sub> composite. This is in accordance with a single-step dehydrogenation of about 3.7 wt. % H<sub>2</sub> from TGA thermogram (Fig.1). Therefore, the dehydrogenation temperature and desorbed hydrogen content of Ca(BH<sub>4</sub>)<sub>2</sub>-MgF<sub>2</sub> composite achieved from DSC-TG-MS results were 390 °C and 3.7 wt. %, respectively.

Not only hydrogen release during dehydrogenation of Ca(BH<sub>4</sub>)<sub>2</sub>-MgF<sub>2</sub> composite was considered, but the formation of hydrofluoric acid (HF) and diborane (B<sub>2</sub>H<sub>6</sub>), which could cause corrosion on various fuel cell compartments and unrecoverable boron loss, were also measured by MS [29]. Fig. 2 shows the negative MS results for the formation of HF and B<sub>2</sub>H<sub>6</sub> during the dehydrogenation of milled Ca(BH<sub>4</sub>)<sub>2</sub>-MgF<sub>2</sub>.

#### 3.2. Reaction mechanisms during dehydrogenation and rehydrogenation

Firstly, the phases formed after drying of Ca(BH<sub>4</sub>)<sub>2</sub>-THF was determined by XRD. From Fig.3, dried Ca(BH<sub>4</sub>)<sub>2</sub> reveals the diffraction peaks corresponding to the mixed phases of  $\alpha$ - and  $\beta$ -Ca(BH<sub>4</sub>)<sub>2</sub>. This is in agreement with the DSC curve (Fig. 1), where the polymorphic transition from  $\alpha$ - to  $\beta$ -Ca(BH<sub>4</sub>)<sub>2</sub> is not observed due to the mixed phases of Ca(BH<sub>4</sub>)<sub>2</sub> (Fig. 1 and section 3.1).

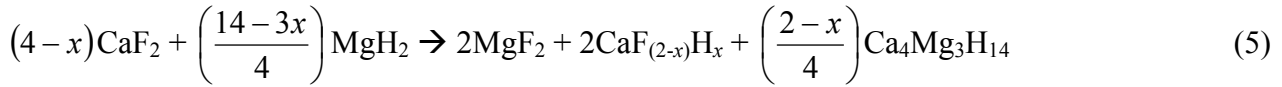
Furthermore, the reaction mechanisms during dehydrogenation and rehydrogenation of Ca(BH<sub>4</sub>)<sub>2</sub>-MgF<sub>2</sub> composite was clarified by SR-PXD and raman spectroscopy. For SR-PXD, during dehydrogenation the milled Ca(BH<sub>4</sub>)<sub>2</sub>-MgF<sub>2</sub> was heated to 390 °C under vacuum and dwelled at 390 °C for 1 h. From Fig. 4, by continuously increasing the temperature of milled Ca(BH<sub>4</sub>)<sub>2</sub>-MgF<sub>2</sub> to about 158 °C and 313 °C, the polymorphic transformation from α- to β-Ca(BH<sub>4</sub>)<sub>2</sub> and the melting of β-Ca(BH<sub>4</sub>)<sub>2</sub> are observed, respectively. At about 280 °C, the diffraction peaks referring to CaF<sub>2</sub> are visible while the intensity of MgF<sub>2</sub> peaks decreases. This implies that fluorine atoms in CaF<sub>2</sub> were obtained from MgF<sub>2</sub> (Fig. 4). Afterward, the reflections of Mg are detected at about 310 °C. However, the status of boron after dehydrogenation of Ca(BH<sub>4</sub>)<sub>2</sub> was not clear. Therefore, the dehydrogenated Ca(BH<sub>4</sub>)<sub>2</sub>-MgF<sub>2</sub> was further examined by raman spectroscopy. Fig. 5 reveals the characteristic peaks corresponding to CaB<sub>6</sub> at 1252, 1117, and 762 cm<sup>-1</sup> together with that of an amorphous boron (a-B) at 1172 cm<sup>-1</sup> [30]. This suggests that the boron compounds generated during dehydrogenation of Ca(BH<sub>4</sub>)<sub>2</sub> were CaB<sub>6</sub> and a-B as in accordance with the previous reports.[10]. On the basis of these results, the dehydrogenation products were CaF<sub>2</sub>, CaB<sub>6</sub>, Mg and a-B.

For rehydrogenation, SR-PXD of the powder sample of dehydrogenated Ca(BH<sub>4</sub>)<sub>2</sub>-MgF<sub>2</sub> obtained from Sievert's-type apparatus was determined by heating to 380 °C under 100 bar H<sub>2</sub>, dwelling at 380 °C for 1 h, and cooling to room temperature. In Fig.6, the first spectrum of the SR-PXD patterns is referring to the dehydrogenated Ca(BH<sub>4</sub>)<sub>2</sub>-MgF<sub>2</sub> collected at room temperature before starting the rehydrogenation process, which takes place only at elevated temperatures. It shows the diffraction peaks of MgH<sub>2</sub> together with those of Mg, MgF<sub>2</sub> and CaF<sub>2</sub>. This suggests that MgH<sub>2</sub> was also one of the dehydrogenation products. It should be mentioned that the disappearance of MgH<sub>2</sub> in Fig. 4 after dehydrogenation might be due to an incomplete dehydrogenation in SR-PXD experiment, which the dwelling time at 390 °C was only 1 h. However, the dehydrogenated Ca(BH<sub>4</sub>)<sub>2</sub>-MgF<sub>2</sub> investigated as the results shown in Fig. 6 was the desorbed material from Sievert's-type apparatus, which the complete dehydrogenation was confirmed. Therefore, the dehydrogenation reaction of Ca(BH<sub>4</sub>)<sub>2</sub>-MgF<sub>2</sub> composite is proposed as followed:

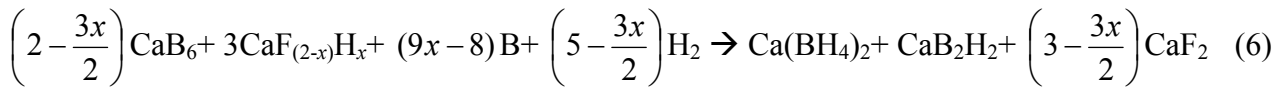


Thereafter, Fig. 6 reveals coarsening and recrystallization of CaF<sub>2</sub>, which could be observed by an increase in the intensity of the corresponding peaks at about 285 °C. By increasing temperature to about 336 °C, the intensity of Mg and MgH<sub>2</sub> peaks decrease significantly while the characteristic peaks of Ca<sub>4</sub>Mg<sub>3</sub>H<sub>14</sub> are detected [25] as well as the slight increase in the intensity of MgF<sub>2</sub> peaks (Fig. 6). Moreover, the diffraction peaks corresponding to CaF<sub>2-x</sub>H<sub>x</sub> arise at about 344 °C. The solid solution of CaF<sub>2-x</sub>H<sub>x</sub> with the same crystal structure as CaF<sub>2</sub> (cubic C1) was previously reported by Brice et al. [31].

The  $\text{CaF}_{2-x}\text{H}_x$  phase is distinguished from that of  $\text{CaF}_2$  by a relatively strong (200) peak at  $2\theta \sim 22.5^\circ$  (Fig. 6), which is not observed in  $\text{CaF}_2$  [6]. Therefore, the reaction during rehydrogenation in the temperature range of 20-340 °C is concluded as given in Eq. (5).



To clarify the reversibility and the further reaction mechanism during rehydrogenation, SR-PXD pattern of  $\text{Ca}(\text{BH}_4)_2\text{-MgF}_2$  composite after rehydrogenation collected at room temperature was considered. Fig. 7 shows the characteristic reflections of both  $\alpha$ - and  $\beta$ - $\text{Ca}(\text{BH}_4)_2$ . This implies the successful rehydrogenation and reversibility of the  $\text{Ca}(\text{BH}_4)_2\text{-MgF}_2$  composite. However, the reflections of  $\text{CaF}_{2-x}\text{H}_x$ , which is assumed to be one of the rehydrogenation products, are disappeared while those of  $\text{CaF}_2$  are well observed as well as those of a possibly new phase ( $\text{CaB}_2\text{H}_2$ ) (Fig. 7). Thus, there could be a consecutive reaction after Eq. (5) during isothermal region (380 °C) of rehydrogenation. With respect to the phases observed in Fig. 5, during rehydrogenation (Fig. 6) and after rehydrogenation (Fig. 7), the following reaction, which could be occurred during the isothermal region (380 °C) of rehydrogenation, is proposed:



On the basis of Eq. (5) and (6), the rehydrogenation products were  $\alpha$ - and  $\beta$ - $\text{Ca}(\text{BH}_4)_2$ ,  $\text{CaB}_2\text{H}_2$ ,  $\text{CaF}_2$ ,  $\text{MgF}_2$ , and  $\text{Ca}_4\text{Mg}_3\text{H}_{14}$  together with  $\text{CaF}_{2-x}\text{H}_x$  as an intermediate phase.

### 3.3. Dehydrogenation, rehydrogenation and cycling efficiency

Owing to the DSC-TG thermogram (Fig. 1), we found that at 375 °C hydrogen desorption was rather fast; that is, an amount of 3.7 wt. %  $\text{H}_2$  was released in only 5 min. To investigate the hydrogen desorption in more detail, the driving force was lowered by increasing the hydrogen back pressure and decreasing the temperature during dehydrogenation. Therefore, the dehydrogenation temperature and pressure chosen for the titration measurements of  $\text{Ca}(\text{BH}_4)_2\text{-MgF}_2$  composite are 330 °C and 0.5 bar  $\text{H}_2$  respectively. As shown in Fig. 8(a), the hydrogen content released after 4 h during the 1<sup>st</sup> dehydrogenation is  $\sim 4.3$  wt.%. This is approximately in agreement with the hydrogen weight loss (3.7 wt.%) from TGA thermogram (Fig. 1). However, it should be noted that the hydrogen storage capacity of the 1<sup>st</sup> dehydrogenation ( $\sim 4.3$  wt.%) is manifestly less than theoretically according to Eq. (4) (6.4 wt.%). This could be explained by the kinetically delayed behavior, which exhibited residual  $\text{MgF}_2$  after dehydrogenation as mentioned in section 3.2 and shown in Fig. 4. Moreover, the temperature of

the stainless steel vial increasing during ball milling could also result in partial hydrogen desorption. However, the hydrogen storage capacity of  $\text{Ca}(\text{BH}_4)_2\text{-MgF}_2$  composite could be improved by altering the weight ratio of  $\text{Ca}(\text{BH}_4)_2\text{:MgF}_2$  from 1:1 to be a suitable value of 4:3, which was obtained from SR-PXD experiments (section 3.2 and Eq. (4)). In the case of rehydrogenation, the experiments were done at 330 °C under 130 bar  $\text{H}_2$  pressure. Fig. 8(a) exhibits that about 5.8 wt.%  $\text{H}_2$  is reabsorbed after 3 h during the 1<sup>st</sup> rehydrogenation. The considerable difference in hydrogen storage capacities obtained from dehydrogenation and rehydrogenation (~1.5 wt.%) could be due to the residual  $\text{MgF}_2$  after dehydrogenation and the dehydrogenation of  $\text{Ca}(\text{BH}_4)_2\text{-MgF}_2$  composite during ball milling as mentioned previously.

For the cycling efficiency, three hydrogen uptake cycles were carried out. From Fig. 8(b), it is found that the hydrogen content absorbed after 2.5 h during the 1<sup>st</sup> and 3<sup>rd</sup> cycles are comparable (5.8 and 5.7 wt.%, respectively), while that of the 2<sup>nd</sup> cycle is only ~ 5.1 wt.% . The inferior hydrogen storage capacity obtained in the 2<sup>nd</sup> cycle could be explained by the slight deviation of the reservoir temperature (~ 0.5 °C) during the 1<sup>st</sup> (or 3<sup>rd</sup>) and 2<sup>nd</sup> cycles. However, the 3<sup>rd</sup> cycle considerably confirms the reliable reversibility of hydrogen content absorbed during cycling by the approaching value to that of the 1<sup>st</sup> cycle (Fig. 8(b)). Besides, we found that the rehydrogenation kinetics of those cycles was approximately equivalent. It should be noted that the  $\text{Ca}(\text{BH}_4)_2\text{-MgF}_2$  composite showed significantly faster kinetics under relatively mild conditions for both dehydrogenation and rehydrogenation as compared to pure  $\text{Ca}(\text{BH}_4)_2$ . For example, the operating temperature and pressure for dehydrogenation and rehydrogenation of  $\text{Ca}(\text{BH}_4)_2\text{-MgF}_2$  composite are 330 °C (0.5 bar  $\text{H}_2$ ) and 330 °C (130 bar  $\text{H}_2$ ), respectively, while those of pure  $\text{Ca}(\text{BH}_4)_2$  based on Eq. (2) are up to 527 °C and 400-440 °C (700 bar  $\text{H}_2$ ), respectively [16]. In addition,  $\text{Ca}(\text{BH}_4)_2\text{-MgF}_2$  composite gave the superior kinetics based on rehydrogenation as compared to  $\text{NbF}_5$ -catalyzed  $\text{Ca}(\text{BH}_4)_2$ . For instant, with respect to the comparable hydrogen storage capacity of 5-6 wt. %, rehydrogenation of  $\text{Ca}(\text{BH}_4)_2\text{-MgF}_2$  composite was completed at 330 °C ( $p(\text{H}_2)=130$  bar) after 2.5 h, while that of  $\text{NbF}_5$ -catalyzed  $\text{Ca}(\text{BH}_4)_2$  was achieved at 420 °C ( $p(\text{H}_2)=90$  bar) after 24 h [6]. Moreover,  $\text{Ca}(\text{BH}_4)_2\text{-MgF}_2$  composite revealed almost 100 % reversibility of absorbed hydrogen content even after three release and uptake cycles, whereas that of  $\text{Ca}(\text{BH}_4)_2\text{-MgH}_2$  composite gave only 60 % reversibility during the first rehydrogenation after 24 h ( $T=350$  °C and  $p(\text{H}_2)=90$  bar) [22]. Besides kinetic improvement, there was the previous report implying that the formation of anion solid solution ( $\text{CaF}_{2-x}\text{H}_x$ ) affected reaction thermodynamics [6]. Therefore, this work suggested that the preparation of  $\text{Ca}(\text{BH}_4)_2\text{-MgF}_2$  composite gave not only the meaningfully kinetic improvement, but the thermodynamic effect caused by  $\text{CaF}_{2-x}\text{H}_x$  formation as an intermediate during rehydrogenation might be also achieved.

#### 4. Conclusion

The composite of  $\text{Ca}(\text{BH}_4)_2\text{-MgF}_2$  was evaluated in regard of its suitability for hydrogen storage. The reaction mechanisms during dehydrogenation and rehydrogenation were investigated by SR-PXD and raman spectroscopy. After the 1<sup>st</sup> dehydrogenation,  $\text{MgF}_2$  was partially residual. Consequently, the hydrogen content released (~4.3 wt.%) was less than that of the theoretical calculation (6.4 wt.%) . In the case of rehydrogenation and cycling efficiency, the hydrogen storage capacities of three cycles were obtained in the range of 5.1-5.8 wt.% after 2.5 h as well as the comparable kinetics. The kinetic destabilization especially for rehydrogenation based on operating temperature and time was obtained. Moreover, the meaningful reproducibility of absorbed hydrogen content was achieved even after three release and uptake cycles. This work implied that the idea to combine RHCs and metal-fluorine catalyzed  $\text{Ca}(\text{BH}_4)_2$  strategies by preparing  $\text{Ca}(\text{BH}_4)_2\text{-MgF}_2$  composite to improve the kinetics of  $\text{Ca}(\text{BH}_4)_2$  was successful. Moreover, the thermodynamics of the system might be also affected by the formation of  $\text{CaF}_{2-x}\text{H}_x$  as the intermediate during rehydrogenation.

#### 5. Acknowledgement

The authors appreciate the financial support from the Alexander von Humboldt Foundation and the European Community in the frame of the FP7 project “FLYHY - Fluorine Substituted High Capacity Hydrides for Hydrogen Storage at low Working Temperatures” (grant agreement no.: N° 226943). .

## References

- [1] Andreasen, A.; Sørensen, M. B.; Burkarl, R.; Møller, B.; Molenbroek, A. M.; Pedersen, A.S.; Vegge, T.; Jensen, T. R. *Appl. Phys. A* **2006**, 82, 515.
- [2] Ngene, P.; Adelhelm, P.; Beale, A. M.; de Jong, K. P.; de Jongh, P. E. *J Phys. Chem. C* **2010**, 114, 6163.
- [3] Bogdanovic, B.; Schwickardi, M. *J. Alloys Compd.* **2002**, 339, 299.
- [4] Chen, P.; Xiong, X.; Lou, J.; Tan, K. L. *Nature* **2002**, 420, 302.
- [5] Züttel, A.; Wenger, P.; Rentsch, S.; Sudan, P.; Mauron, Ph.; Emmenegger, Ch. *J. Power Sources* **2003**, 118, 1.
- [6] Kim, J. -H.; Shim, J. -H.; Cho, Y. W. *J. Power Sources* **2008**, 181, 140.
- [7] Wiber, E.; Hartwimmer, R. *Z. Naturforsch., B: Chem. Sci.* **1955**, 10, 295.
- [8] Wiber, E.; Noth, H.; Hartwimmer, R. *Z. Naturforsch., B: Chem. Sci.* **1955**, 10, 292.
- [9] Mikheeva, V. I.; Titov, L. V. *Zh. Neorg. Khim.* **1964**, 9, 789.
- [10] Miwa, K.; Aoki, M.; Noritake, T.; Ohba, N.; Nakamori, Y.; Towata, Shin-ichi; Züttel, A.; Orimo, Shin-ichi *Phys. Rev. B* **2006**, 74, 155122.
- [11] Majzoub, E. H., Rönnebro, E. *J. Phys. Chem. C* **2009**, 113, 3352.
- [12] George, L., Drozd, V., Saxena, S. K., Bardaji, E. G., Fichtner, M. *J Phys. Chem. C* **2009**, 113, 15087.
- [13] Buchter, F., Lodziana, Z., Remhof, A., Friedrichs, O., Borgschulte, A., Mauron, Ph., Züttel, A., Sheptyakov, D., Barkhordarian, G., Bormann, R., Chlopek, K., Fichtner, M., Sørby, M., Riktor, M., Hauback, B., Orimo, S., *J. Phys. Chem. B* **2008**, 112, 8042.
- [14] Lee, Y.-S., Kim, Y., Cho, Y. W., Shapiro, D., Wolverton, C., Ozolins, V. *Phys. Rev. B* **2009**, 79, 104107.
- [15] Filinchuk, Y., Rönnebro, E., Chandra, D. *Acta Mat.* **2009**, 57, 732.
- [16] Kim, J. -H.; Jin, S.-A.; Shim, J.-H.; Cho, Y. W. *J. Alloys Compd.* **2008**, 461, L20.
- [17] Wang, L.-L., Graham, D. D., Robertson, I. M., Johnson, D. D. *J. Phys. Chem. C* **2009**, 113, 20088.
- [18] Frankcombe, T. J. *J. Phys. Chem. C* **2010**, 114, 9503.
- [19] Riktor, M. D., Sørby, H. M., Chlopek, K., Fichtner, M., Buchter, F., Züttel, A., Hauback, B. C. *J. Mater. Chem.* **2007**, 17, 4939.
- [20] Riktor, M. D., Sørby, H. M., Chlopek, K., Fichtner, M., Buchter, F., Hauback, B. C. *J. Mater. Chem.* **2009**, 19, 2754.
- [21] Aoki, M., Miwa, K., Noritake, T., Ohba, N., Matsumoto, M., Li, H. -W., Nakamori, Y., Towata, S., Orimo, S. *Appl. Phys. A: Mater. Sci. Proc.* **2008**, 92, 601.

- [22] Kim, Y.; Reed, D.; Lee, Y. -S.; Lee, J. Y.; Shim, J. -H.; Book, D.; Cho, Y. W. *J. Phys. Chem. C* **2009**, 113, 5865.
- [23] Rönnebro, E.; Majzoub, E. H. *J. Phys. Chem. B* **2007**, 111, 12045.
- [24] Dornheim, M.; Doppiu, S.; Barkhordarian, G.; Boesenberg, U.; Klassen, T.; Gutfleisch, O.; Bormann, R. *Scr. Mater.* **2007**, 56, 841.
- [25] Barkhordarian, G.; Jensen, T. R.; Doppiu, S.; Bösenberg, U.; Borgschulte, A.; Gremaud, R.; Cerenius, Y.; Dornheim, M.; Klassen, T.; Bornamm, R. *J. Phys. Chem. C* **2008**, 122, 2743.
- [26] Kim, J. -H.; Jin, S. -A.; Shim, J. -H.; Cho, Y. W. *Scr. Mater.* **2008**, 58, 481.
- [27] Cerenius, Y.; Ståhl, K.; Svensson, LA.; Ursby, T.; Oskarsson, Å.; Albertsson, J.; Liljas, A. *J. Synchrotron. Rad.* **2003**, 7, 203.
- [28] Bösenberg, U.; Doppiu, S.; Mosegaard, L.; Barkhordarian, G.; Eigen, N.; Borgschulte, A.; Jensen, T. R.; Cerenius, Y.; Gutfleisch, O.; Klassen, T.; Dornheim, M.; Bormann, R. *Acta Mater.* **2007**, 55, 3951.
- [29] Brinks, H. W.; Fossdal, A.; Hauback, B. C. *J. Phys. Chem. C* **2008**, 112, 5658.
- [30] Shirai, K.; Thorpe, MF. *Phys. Rev. B* **1997**, 55, 12244.
- [31] Brice, J. -F.; Courtios, A.; Aubry, J. *J. Solid State Chem.* **1978**, 24, 381.

## Figure captions

Fig. 1. Simultaneous TGA-DSC-MS curves of milled  $\text{Ca}(\text{BH}_4)_2\text{-MgF}_2$ .

Fig. 2. MS spectra of milled  $\text{Ca}(\text{BH}_4)_2\text{-MgF}_2$ .

Fig. 3. XRD spectra of dried  $\text{Ca}(\text{BH}_4)_2$

Fig. 4. SR-PXD spectra of milled  $\text{Ca}(\text{BH}_4)_2\text{-MgF}_2$  under vacuum with the temperature program of (i) heating from 25-390 °C; and (ii) dwelling at 390 °C for 1 h.

Fig. 5. Raman spectra of  $\text{CaB}_6$  (a) and dehydrogenated  $\text{Ca}(\text{BH}_4)_2\text{-MgF}_2$  (b).

Fig. 6. SR-PXD spectra of dehydrogenated  $\text{Ca}(\text{BH}_4)_2\text{-MgF}_2$  under 100 bar  $\text{H}_2$  with the temperature program of (i) heating from 25-380 °C; and (ii) dwelling at 380 °C for 1 h.

Fig. 7. SR-PXD spectra of rehydrogenated  $\text{Ca}(\text{BH}_4)_2\text{-MgF}_2$  at room temperature.

Fig. 8. Dehydrogenation and rehydrogenation isotherms of milled  $\text{Ca}(\text{BH}_4)_2\text{-MgF}_2$  at 330 °C (0.5 bar  $\text{H}_2$ ) and 330 °C (130 bar  $\text{H}_2$ ), respectively (a) and cycling efficiency (b).

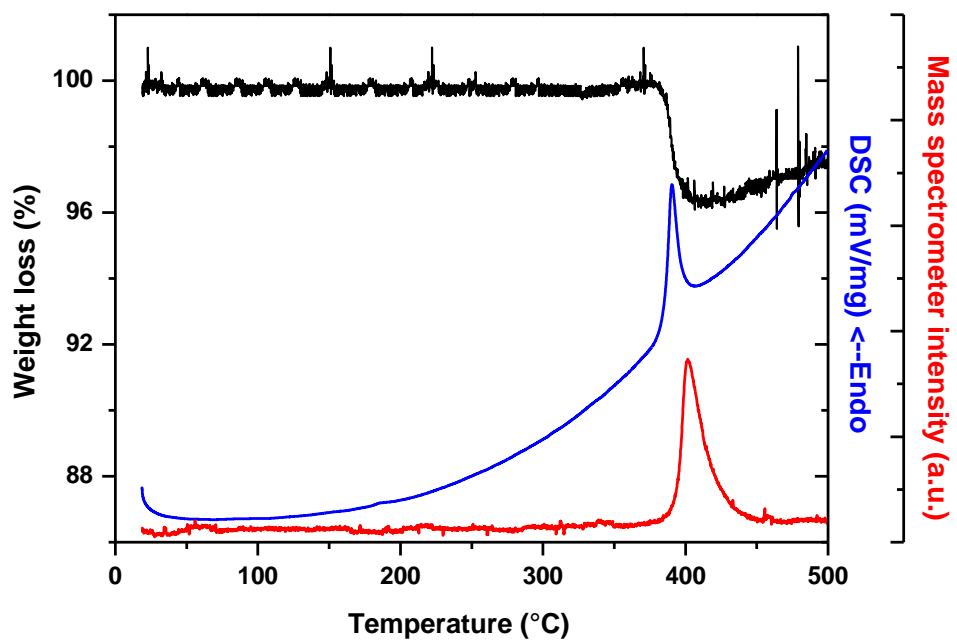


Fig. 1

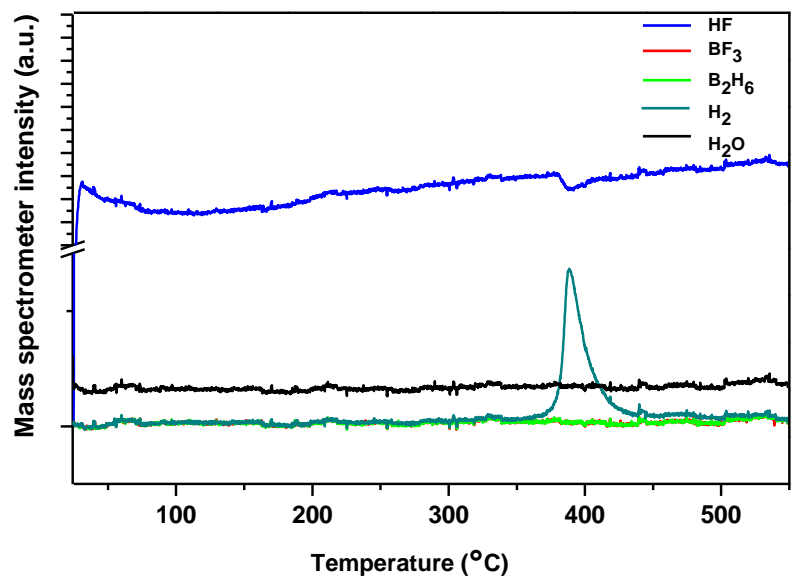


Fig. 2

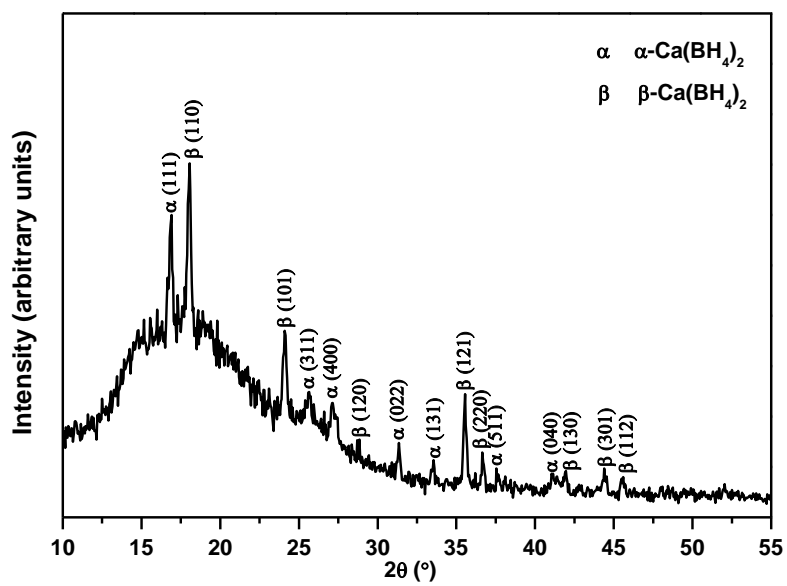
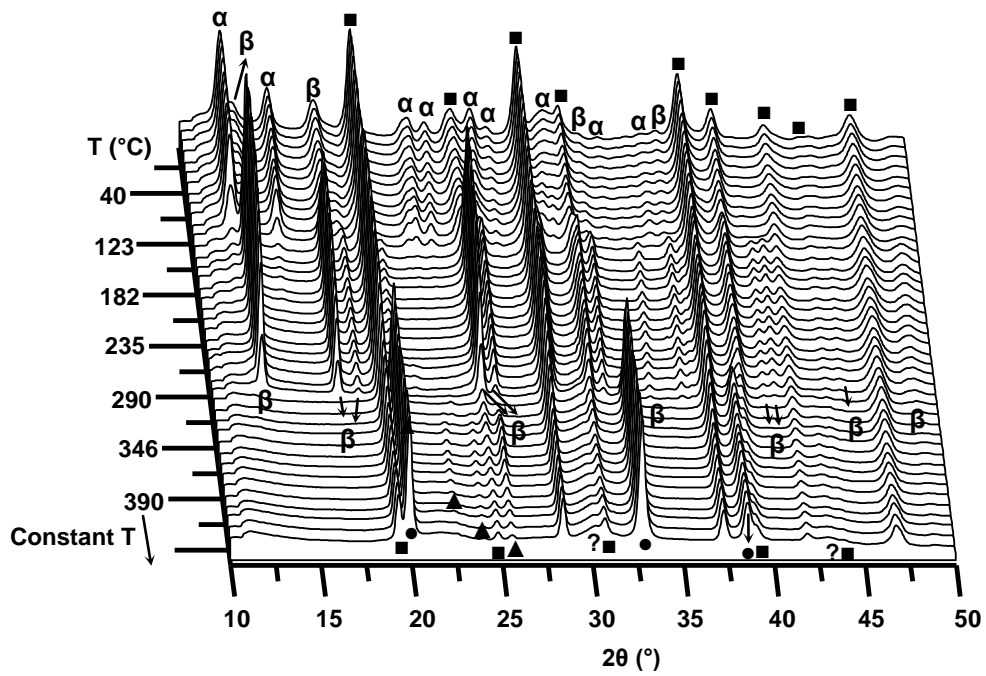


Fig. 3



$\alpha$   $\alpha\text{-Ca}(\text{BH}_4)_2$      $\beta$   $\beta\text{-Ca}(\text{BH}_4)_2$     ■  $\text{MgF}_2$   
 ▲  $\text{Mg}$                       ●  $\text{CaF}_2$                       ? unknown

Fig. 4

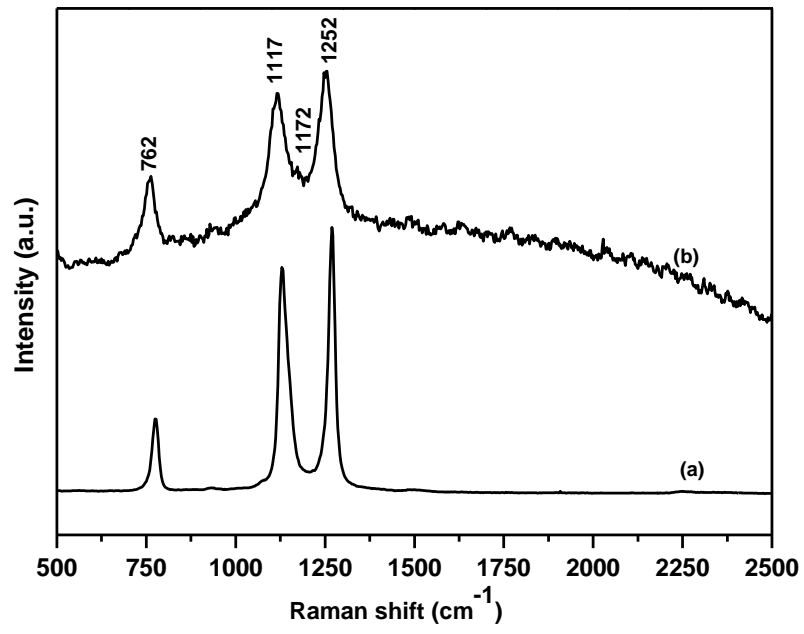
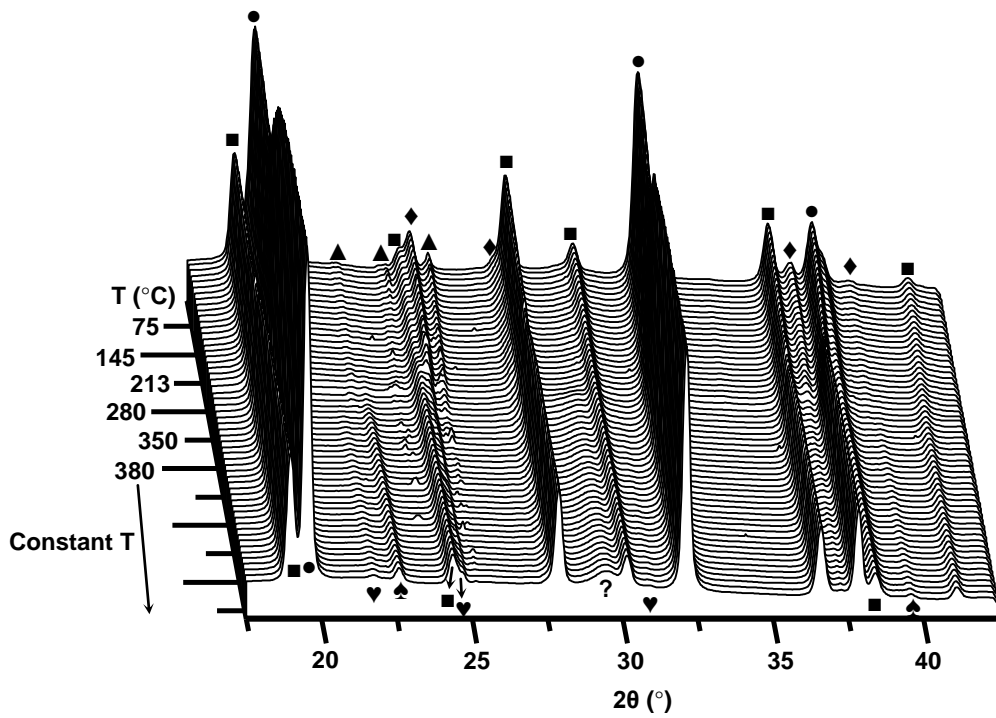


Fig. 5

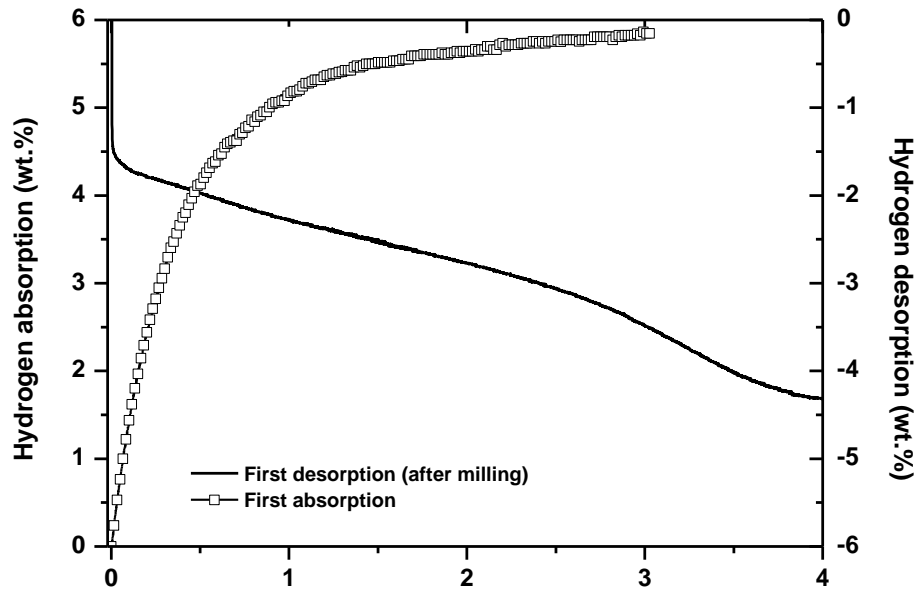


- |   |                                |                  |                  |
|---|--------------------------------|------------------|------------------|
| ■ $\text{MgF}_2$                        | ▲ $\text{Mg}$                  | ● $\text{CaF}_2$ | ◆ $\text{MgH}_2$ |
| ♣ $\text{Ca}_4\text{Mg}_3\text{H}_{14}$ | ▼ $\text{CaF}_{2-x}\text{H}_x$ | ? unknown        |                  |

Fig. 6



(a)



(b)

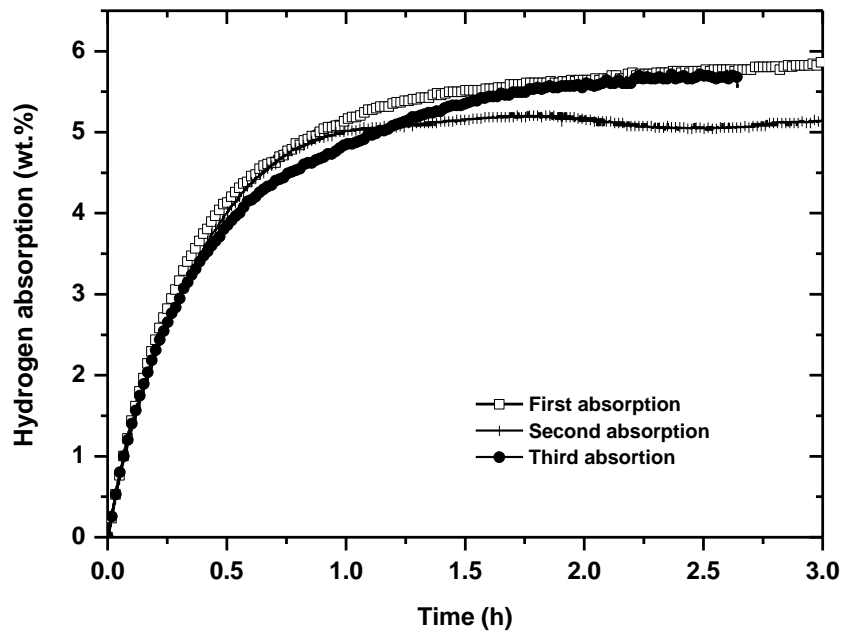


Fig. 8